

Quantum teleportation between two mesoscopic objects: a photonic pulse and an atomic ensemble

Jacob Sherson¹, Hanna Krauter¹, Rasmus K. Olsson¹, Brian Julsgaard¹, Klemens Hammerer², Ignacio Cirac², and Eugene S. Polzik¹

¹⁾*Niels Bohr Institute, Danish Quantum Optics Center – QUANTOP, Copenhagen University, Blegdamsvej 17, Copenhagen Ø, Denmark.*

²⁾*Max Planck Institute for Quantum Optics, Hans-Kopfermann-Str. 1, Garching, Germany*

Quantum teleportation¹ is one of the main paradigms in quantum information science. It is an important ingredient in distributed quantum networks², and can also serve as an elementary operation in quantum computers³. In this paper we demonstrate for the first time quantum teleportation between two objects of different nature: a pulse of light and a material object. A quantum state encoded in a mesoscopic light pulse is teleported onto an atomic ensemble containing 10^{12} Cesium atoms. The teleportation is performed at a distance of 0.5m, and this distance can be increased limited primarily by losses in the transmission of the light. The teleportation is deterministic, with a fidelity of 0.58 ± 0.02 for coherent states with a mean photon number of 20 and a fidelity of 0.61 ± 0.02 for states with 5 photons - significantly higher than any classical state transfer can possibly achieve⁴. Quantum teleportation between the carrier of information – light - and the storage and processing medium – atoms - is a new step towards distributed quantum networks.

Quantum teleportation - a disembodied transfer of a quantum state with the help of distributed entanglement - was proposed in a seminal paper¹. It was demonstrated for

the first time as teleportation of a quantum state of light on another light beam⁵⁻⁷. Pure photonic teleportation has been further developed by several groups including demonstration of long distance qubit teleportation using optical relays⁸ and high fidelity teleportation and entanglement swapping for continuous variables⁹. Recently a new breakthrough – the teleportation of a quantum state of a single material particle: a trapped ion - was reported by two groups^{10,11}. In this paper we demonstrate teleportation with advances in three directions: it is the first teleportation between different species, light and matter; it involves a large atomic object consisting of hundreds of billions of atoms; and finally, teleportation onto a material object is performed at a distance several orders of magnitude larger than demonstrated previously^{10,11}.

The generic protocol of quantum teleportation begins with creation of a pair of entangled objects which are shared by two parties, Alice and Bob. This step establishes a quantum link between them. Alice receives an object to be teleported and performs a joint measurement on her entangled object and on the object of teleportation. The results of this measurement are then communicated via a classical communication channel to Bob, who uses them to perform local operations on his entangled object, thus completing the process of teleportation. In our experiment a pair of entangled objects is created by sending a pulse of light through an atomic sample (see Fig.1). As a result of the interaction light and atoms become entangled. Alice receives the entangled pulse of light, whereas Bob has the atoms. In the experiment Alice is positioned at 0.5 m from Bob but she could just as well be at a considerably longer distance from Bob, limited only by the propagation efficiency of light and the lifetime of the atomic object. On Alice's site the entangled pulse is mixed with the pulse to be teleported on a 50/50 beamsplitter. Measurements in the two output ports of the beamsplitter are then carried out and the results are transferred back to Bob as classical photocurrents. Bob performs local operations on his atoms to complete the teleportation protocol. Finally, the state of atoms is analyzed to confirm that the teleportation has been successful.

The experiment follows the recent proposal for light-to-atoms teleportation¹² using multimode entanglement of light with an atomic ensemble placed in a magnetic field. We describe teleportation in the language of canonical variables¹³; this provides a common description for light and atoms, and allows for a complete tomographic characterization of the states. The atomic object is a gas sample of Cesium atoms in a paraffin coated cell¹⁴⁻¹⁸. Atoms are initially prepared in a coherent spin state by optical pumping along the x axis into the sublevel $F = 4, m_F = 4$ (see Fig.1) of the ground state with the collective ensemble angular momentum $\langle \hat{J}_x \rangle = J_x = 4N_{atoms}$, and the transverse projections with minimal quantum uncertainties, $\langle \delta J_y^2 \rangle = \langle \delta J_z^2 \rangle = \frac{1}{2} J_x$. A homogeneous magnetic field is applied along the x direction. Changing to the frame rotating at the Larmor frequency Ω and introducing the canonical variables for the transverse atomic spin components¹², we obtain $\hat{X}_A = \hat{J}_y^{rot} / \sqrt{J_x}$, $\hat{P}_A = \hat{J}_z^{rot} / \sqrt{J_x}$ which obey the usual commutation relation $[\hat{X}_A, \hat{P}_A] = i$. The state of the light pulse is described in the language of single mode canonical operators \hat{Y}, \hat{Q} . The quantum teleportation is equivalent to a faithful transfer of these non-commuting, and hence not simultaneously measurable, quantities onto the atomic spin variables \hat{X}_A, \hat{P}_A .

Teleportation begins when a strong y -polarized off-resonant pulse of light with frequency ω is sent through Bob's atomic ensemble. The atomic level scheme and coupling of levels to the optical fields is shown in the inset in Fig.1. At Alice's location, the transmitted pulse, which is now entangled with atoms¹², is mixed on a beamsplitter with the object of teleportation - a few-photon coherent pulse with frequency $\omega + \Omega$ polarized along the y direction. A standard method for measuring the canonical variables for light is a homodyne detection followed by the normalization to the vacuum (shot) noise of light⁷. In our experiment the strong pulse, besides driving the entangling interaction, also plays the role of a local oscillator for homodyne balanced detection of quantum fields (see the Methods section).

The object of teleportation is generated by applying a weak modulation at the frequency $\Omega = 322\text{kHz}$ to an electro-optical modulator (EOM) in the signal path (see Fig.1). The EOM shifts the input vacuum state of the mode to create a coherent state with a certain amplitude and phase. The sideband quadrature operators to be teleported, $\hat{Y} = \frac{1}{\sqrt{2}}(\hat{Y}_s + \hat{Q}_c)$, $\hat{Q} = -\frac{1}{\sqrt{2}}(\hat{Y}_c - \hat{Q}_s)$, can be expressed via the $\sin(\Omega t)$ and $\cos(\Omega t)$ components $\hat{Y}_s, \hat{Q}_s, \hat{Y}_c, \hat{Q}_c$. In one of the outputs of the beam splitter (Fig.1) the components that are in phase with the strong pulse $\hat{y}_{c,s} = \frac{1}{\sqrt{2}}(\hat{y}_{c,s}^{out} + \hat{Y}_{c,s})$ are measured via a polarization homodyne measurement of the Stokes parameter \hat{S}_2 , whereas the out-of-phase components $\hat{q}_{c,s} = \frac{1}{\sqrt{2}}(\hat{q}_{c,s}^{out} - \hat{Q}_{c,s})$ are measured via the Stokes parameter \hat{S}_3 in the other output (see the Methods section for details). The $\sin(\Omega t)$ and $\cos(\Omega t)$ components are measured by processing photocurrents with lock-in amplifiers. The input state quadratures, \hat{Y}, \hat{Q} , are now contained in the following two combinations of the measured quantities $\hat{y}_s - \hat{q}_c = \frac{1}{\sqrt{2}}(\hat{y}_s^{out} - \hat{q}_c^{out}) + \hat{Y}$, $\hat{y}_c + \hat{q}_s = \frac{1}{\sqrt{2}}(\hat{y}_c^{out} + \hat{q}_s^{out}) - \hat{Q}$. The operators $\hat{y}_{c,s}^{out}, \hat{q}_{c,s}^{out}$ describe the x -polarized mode of the field after the interaction with the atomic ensemble. Those modes are filled with coherent forward scattering from the atomic ensemble, as shown in¹²:

$$\begin{aligned}
 \hat{y}_c^{out} &= \left\{ \hat{y}_c^{in} + \frac{\kappa^2}{4} \hat{q}_s^{in} + \frac{\kappa^2}{4\sqrt{3}} v_s \right\} + \frac{\kappa}{\sqrt{2}} \hat{P}_A^{in}, & \hat{q}_{s,c}^{out} &= \hat{q}_{s,c}^{in} \\
 \hat{y}_s^{out} &= \left\{ \hat{y}_s^{in} - \frac{\kappa^2}{4} \hat{q}_c^{in} + \frac{\kappa^2}{4\sqrt{3}} v_c \right\} - \frac{\kappa}{\sqrt{2}} \hat{X}_A^{in}
 \end{aligned}
 \tag{1}$$

The terms in curly brackets in the equations for \hat{y} represent contributions coming from the input state of the entangling pulse¹². The canonical operators $\hat{y}_{c,s}^{in}, \hat{q}_{c,s}^{in}, v_{s,c}$ represent different input vacuum modes. The terms containing \hat{P}_A^{in} and \hat{X}_A^{in} describe the imprint of the atomic state on the light which leads to the entanglement of light and atoms. The physical mechanism of this entanglement is the quantum Faraday effect^{14,15}. Equations (1) present a complex type of atoms-light entanglement. Although this type of

entanglement differs from the Einstein-Podolsky-Rosen (EPR) type which is optimal for quantum teleportation, it is very close to optimal under our experimental conditions¹².

The light-atoms coupling constant $\kappa = a_1 \sqrt{N_{ph} N_{at} F \sigma \Gamma} / A \Delta$, where σ is the dipole cross section, a_1 - vector polarizability, $\Gamma = 2.5 \text{ MHz}$ - natural linewidth (HWHM) of the transition, $N_{ph} = 4 \cdot 10^{13}$ - the number of the y-polarized photons in the strong entangling pulse, $\Delta = 825 \text{ MHz}$ - the detuning of light from the atomic resonance, and $A = 4.4 \text{ cm}^2$ - the cross section of the atomic sample, has been discussed in detail previously^{12,14-18}. In the experiment we choose κ to be close to the optimal value¹² of unity by adjusting the number of atoms in the cell. Note that a very large photon number N_{ph} is used in the classical y-polarized mode in order to achieve coherently enhanced atoms-light interaction.

The atomic ensemble spin variables are transformed by the interaction with light in the following way¹²:

$$\langle \text{fd} \rangle \quad \hat{X}_A^{\text{out}} = \hat{X}_A^{\text{in}} + \frac{\kappa}{\sqrt{2}} \hat{q}_c^{\text{in}}, \quad \hat{P}_A^{\text{out}} = \hat{P}_A^{\text{in}} + \frac{\kappa}{\sqrt{2}} \hat{q}_s^{\text{in}} \quad (2)$$

again clearly demonstrating entanglement of the photonic and atomic degrees of freedom. The second terms in eq.(2) describe the imprint of the light state onto atoms via the dynamic Stark effect, as demonstrated in the context of quantum memory¹⁴.

The measurements of operators $\hat{y}_{c,s}$ and $\hat{q}_{c,s}$ are carried out at Alice's location with polarization detectors yielding the results $y_{c,s}$ and $q_{c,s}$. Operationally these numbers are properly normalized integrals over a pulse duration of corresponding photocurrents (see the Methods section for details). As shown in Fig.1 the photocurrents are combined and converted into two classical feedback signals proportional to $y_s - q_c$ and $y_c + q_s$ which are sent from Alice to Bob. The collective atomic spin variables at Bob's site are then shifted by applying pulses of an auxiliary magnetic field with frequency Ω and

amplitude proportional to the feedback signals. These pulses rotate the collective spin of atoms such that $\hat{X}_A^{tele} = \hat{X}_A^{out} + g(y_s - q_c)$, $\hat{P}_A^{tele} = \hat{P}_A^{out} - g(y_c + q_s)$, where g is the feedback gain. This step completes the teleportation protocol.

To prove that we have successfully performed quantum teleportation we have to determine the fidelity of the teleported state with respect to the input state. Towards this end, we send a second - verifying - strong pulse of y-polarized light through atoms after the teleportation is completed. From this measurement we reconstruct the atomic operators \hat{X}_A^{tele} and \hat{P}_A^{tele} . The fidelity is the overlap of the input state and the teleported state averaged over the input state distribution. For a coherent input state of light with mean quadrature operators \bar{Y} , \bar{Q} and vacuum variances, and for a Gaussian teleported state of atoms with mean values \bar{X}_A^{tele} , \bar{P}_A^{tele} and variances σ_X^2 , σ_P^2 , the state overlap is given by

$$O = 2\exp\left(-(\bar{Y} - \bar{X}_A^{tele})^2/(1 + 2\sigma_X^2) - (\bar{Q} - \bar{P}_A^{tele})^2/(1 + 2\sigma_P^2)\right)/\sqrt{(1 + 2\sigma_X^2)(1 + 2\sigma_P^2)}.$$

The mean values of the input state quadratures are determined from the results of the first strong pulse outputs: $\bar{y}_s - \bar{q}_c = \bar{Y}$ and $\bar{y}_c + \bar{q}_s = \bar{Q}$. The mean values and the variances of the teleported atomic state are determined from the second (verifying) pulse measurements. Using eq.(1,2) and the beam splitter relations we find that the measurement of the verifying pulse on the S_2 detector yields the following mean values:

$$\bar{y}_c^{ver} = \frac{\kappa}{2}\bar{P}_A^{tele} = \frac{g\kappa}{2}\bar{Q}, \quad \bar{y}_s^{ver} = \frac{\kappa}{2}\bar{X}_A^{tele} = \frac{g\kappa}{2}\bar{Y}. \quad \text{The value of } \kappa = 0.93 \text{ is determined}$$

from the projection noise measurement (see the Methods section) which allows us to determine g from the measurements of mean values. In Fig.2a \hat{y}_c^{ver} is plotted as a function of \hat{Q} for 10,000 teleportation attempts for a slowly scanned input state phase. From the linear fit to this distribution we find g which can then be tuned to a desired value electronically. Results plotted in Fig. 2a along with similar results for another quadrature $\bar{y}_s(\bar{Y})$ present the proof of the successful *classical* transfer of the mean values of the quantum mechanical operators \hat{Y}, \hat{Q} of light onto atoms.

To verify the success of the *quantum* teleportation we have to determine the variances of the two atomic operators which now contain the teleported input light state. Fig. 2b shows the results $\hat{y}_c^{ver}, \hat{y}_s^{ver}$ for 250 teleportation runs for a fixed input state of light with $\bar{n} = 5$. Making use of Eq.(1) and the beamsplitter relations we find the atomic state variances from this distribution to be:

$$\sigma_{x,p}^2 = \frac{4}{\kappa^2} \left[\text{Var}\{\hat{y}_{c,s}\} - \frac{\kappa^4}{48} - \frac{1}{2} \right] = 1.22 \pm 0.03, \text{ with the experimental values}$$

$\kappa = 0.93 \pm 0.02$. The error bar is calculated from the statistical uncertainty of the measurement of the projection noise of atoms and the shot noise of light. This value is to be compared with $\frac{3}{2}$ which corresponds to the 3 units of vacuum noise, the lowest noise that can be achieved via a classical transfer of coherent states^{4,7}. The fidelity of the quantum teleportation is then $F = 0.58 \pm 0.02$ which is significantly higher than the best classical fidelity of 0.5 for an infinite set of coherent states⁴(see Supplementary Methods for the calculation of the standard deviation of the fidelity).

In Fig.3 we show the tomographically reconstructed teleported coherent state with the mean photon number $\bar{n} = 5$. Due to the Gaussian character of the state, the knowledge of the means and the variances of two quadrature phase operators is sufficient for the reconstruction.

The question then arises: how many photons can be contained in a state that can be reliably teleported? The upper limit in our experiment is set by the fluctuations and uncertainty of the classical gain and the coupling parameter κ . Obviously if the set of quantum states to be teleported contains large photon number states, fluctuations of the classical gain will lead to large uncontrolled displacements of the teleported state with respect to the input state, and hence to the decrease in the fidelity. We have run several series of teleportation experiments with mesoscopic photon numbers $\bar{n} = 0$ (vacuum), $\bar{n} = 5, 20, 45, 180, 500$. The benchmark classical fidelity⁴ for a Gaussian distribution of

coherent states with the width $\langle n \rangle$ is given by $F_n^{class} = \frac{\langle n \rangle + 1}{2\langle n \rangle + 1}$. The experimental

quantum teleportation yields the results which are significantly higher than the corresponding classical benchmark values: $F_2 = 0.64 \pm 0.02$; $F_5 = 0.61 \pm 0.02$; $F_{10} = 0.59 \pm 0.02$; $F_{20} = 0.58 \pm 0.02$; $F_{300} = 0.56 \pm 0.02$. The effect of the atomic decoherence and losses of light on the teleported state has been modeled in¹². For our experimental values this model predicts, e.g. $F_5 = 0.66$, which is close to the observed value.

Note that the size of the atomic object onto which the teleportation is performed contains hundreds of billions of atoms. However, the number of excitations in the ensemble, of course, corresponds to the number of photons in the initial state of light. Those excitations are coherently distributed over the entire ensemble.

Another question is the applicability of this teleportation protocol to the teleportation of a light qubit. In the Supplementary Notes we give the derivation of the predicted qubit fidelity, F_q , based on the performance of our teleportation protocol for coherent states. In the absence of losses and decoherence, $F_q = 0.74$ - significantly higher than the best classical fidelity for a qubit of 0.67. In order to demonstrate the light qubit teleportation, a source generating such a qubit in a temporal, spectral and spatial mode compatible with an atomic target is required. First steps towards generation of an atom-compatible qubit state of light have been made using atomic ensembles¹⁹⁻²¹, single atoms in a cavity^{22,23}, and a photon subtracted squeezed state²⁴.

Further improvement of the present teleportation protocol can be achieved via performing more complex measurements on the transmitted light. As shown in¹² and in the Supplementary Notes, fidelity approaching unity for any input state can be achieved if such measurements are combined with using a squeezed entangling pulse.

Methods.

Calibration and measurement techniques. Physically we perform measurements of the Stokes operators of light by two sets of balanced homodyne detectors as shown in Fig.1. The measurements on the first pulse represent the generalized Bell measurement. The same measurements on the second (verifying) pulse allow us to determine the teleported atomic state by performing quantum state tomography. The relevant $\cos(\Omega t)$ and $\sin(\Omega t)$ modulation components of the Stokes operators are measured by processing the corresponding photocurrents with lock-in amplifiers. The Stokes operators of interest are \hat{S}_2 - which is the difference between photon fluxes in the modes polarized at $\pm 45^\circ$ to the vertical axis, and \hat{S}_3 - is the corresponding quantity for the left- and right-hand circular polarizations.

Calibration of the measurement of canonical variables for light is based on measurements of the shot (vacuum) noise level. We measure the Stokes parameters for the x -polarization mode in a vacuum state. The linear dependence of the variance of the measured photocurrents on the optical power of the strong pulse proves that the polarization state of light is, in fact, shot (vacuum) noise limited. All other measurements of \hat{S}_2, \hat{S}_3 are then normalized to this shot noise level yielding the canonical variables as $y_c = \frac{1}{\sqrt{2} \int_0^T d\tau \cos(\Omega t) S_2^{\text{vacuum}}(\tau)} \int_0^T d\tau \cos(\Omega t) S_2(\tau)$ and similarly

for $q_c(S_3)$ and the $\sin(\Omega t)$ components.

Next we need to calibrate the atomic coherent (projection) noise level. Whereas balanced homodyne detection for light has become an established technique for determination of the vacuum state⁷, a comparable technique for atoms is a relatively recent invention. In this paper we utilize the same procedure as used in our previous experiments on the atoms-light quantum interface^{14,15}. We use the fact that the vacuum

(projection) noise level for collective atomic spin states in the presence of a bias magnetic field can be determined by sending a pulse of light through *two* identical atomic ensembles with oppositely oriented macroscopic spin orientation. We therefore insert a second atomic cell in the beam. As described in detail in¹⁵, the transmitted light state in this experiment is given by $\hat{y}_c^{out} = \hat{y}_c^{in} + \frac{\kappa}{\sqrt{2}}(\hat{P}_{atom1} + \hat{P}_{atom2}) = \hat{y}_c^{in} + \kappa\hat{P}_{total}$, where \hat{P}_{total} is the spin canonical variable for the entire 2-cell atomic sample. Intuitively this equation can be understood by noting that terms proportional to κ^2 in Eq. (1) cancel out for propagation through two oppositely oriented ensembles. A similar equation holds for \hat{y}_s^{out} with substitution of \hat{X}_{total} for \hat{P}_{total} . The results for $Var(\hat{y}_{c,s}^{out})$ as a function of the number of atoms are shown in the figure in the Supplementary Methods. The fact that the points lie on a straight line, along with the independent measurement of the degree of spin polarization above 0.99, proves^{14,15} that we are indeed measuring the vacuum (projection) noise of the atomic ensemble. κ^2 for different atomic numbers is then calculated from the graph (see Supplementary Methods). Its values are in good agreement with the theoretical calculation¹⁸ according to $\kappa = a_1 \sqrt{N_{ph} N_{at} F \sigma \Gamma} / A \Delta$. In the experiment we monitor the number of atoms by sending a weak off-resonant probe pulse along the direction x and measuring the Faraday rotation angle proportional to the collective macroscopic spin of the ensemble $J_x = 4N_{atoms}$. This Faraday angle is monitored throughout the teleportation experiment, so that the value of κ^2 is known at every stage.

Decoherence and losses. The main sources of imperfections are decoherence of the atomic state and reflection losses of light. Calculations of the effect of dissipation on the fidelity carried out in¹² yield predictions comparable to the obtained experimental results. Dissipation also affects the experimental state reconstruction procedure. The main effect of the light losses $\varepsilon = 0.09$ is that it modifies kappa κ into $\kappa \Rightarrow \kappa\sqrt{1-\varepsilon}$. However, this modified κ is, in fact, exactly the parameter measured in the two-cell

calibration experiment described above, so no extra correction is due to these losses. There is also a small amount of electronic noise of detectors which can be treated as an extra vacuum contribution to the input state.

The rate of atomic decoherence in the absence of interaction with light is very low corresponding to the coherence lifetime of $40msec$. However, the verifying pulse causes a much faster decoherence of the atomic state via the process of light-induced collisions¹⁶⁻¹⁸. This leads to the reduction in the mean spin values $J_{y,z}$ according to $e^{-\beta\tau}$. We must adjust the gain calibration to take this small but still important effect into account. The decay constant $\beta = 0.09msec^{-1}$ of the mean atomic spin orientation in the presence of the probe light is measured in a separate experimental run. As a result of this decay the verifying pulse measures reduced mean values $\bar{y}_c = \frac{1}{2} g \kappa e^{-\beta\tau} \bar{Q}$, $\bar{y}_s = \frac{1}{2} g \kappa e^{-\beta\tau} \bar{Y}$ as compared to the teleported mean values, where $\tau = 1msec$ is the time interval from the beginning of the verifying pulse to its center yielding $e^{-\beta\tau} = 0.91$. Thus the unity gain g is determined from the condition that the slope in Fig.2a is $\frac{\bar{y}_c}{\bar{Q}} = \frac{1}{2} g \kappa e^{-\beta\tau} = \frac{1}{2} \cdot 1 \cdot 0.93 \cdot 0.91 = 0.42$.

1. Bennett C.H., Brassard G., Crepeau C., Jozsa R., Peres A., Wootters W.K. , Teleporting an unknown quantum state via dual classical and Einstein-Podolsky-Rosen channels. *Phys. Rev. Lett.* **70**, 1895 (1993)
2. Briegel H. J., Dur W., Cirac J.I., and Zoller P., Quantum Repeaters: The Role of Imperfect Local Operations in Quantum Communication, *Phys. Rev. Lett.* **81**, 5932 (1998).
3. D. Gottesman and I. Chuang, Demonstrating the viability of universal quantum computation using teleportation and single-qubit operations. *Nature* **402**, 390 (1999).

4. K. Hammerer, M.M. Wolf, E.S. Polzik, J.I. Cirac, Quantum benchmark for storage and transmission of coherent states. *Phys. Rev. Lett.* **94**,150503 (2005)
5. D. Bouwmeester, Pan J. W., Mattle K., Eibl M., Weinfurter H., Zeilinger A., *Nature* **390**, 575 (1997)
6. D. Boschi, Branca S., De Martini F., Hardy L., Popescu S., *Phys. Rev. Lett.* **80**, 1121 (1998)
7. Furusawa A., Sorensen J.L., Braunstein S.L., Fuchs C.A., Kimble H.J., and Polzik E.S., Unconditional quantum teleportation. *Science*, **282**, 706 (1998).
8. de Riedmatten H., Marcikic I., Tittel W., Zbinden H., Collins A., Gisin N. Long distance quantum teleportation in a quantum relay configuration. *Phys. Rev. Lett.*, **92**, 047904 (2004).
9. Takei N., Yonezawa H., Aoki T., Furusawa A. High-fidelity teleportation beyond the no-cloning limit and entanglement swapping for continuous variables. *Phys. Rev. Lett.* **94**, 220502 (2005).
10. Barrett M.D., Chiaverini J., Schaetz T., Britton J., Itano W.M., Jost J.D., Knill E., Langer C., Leibfried D., Ozeri R., Wineland D.J. Deterministic quantum teleportation of atomic qubits, *Nature* **429**, 737-739 (2004).
11. Riebe M., Haffner H., Roos C.F., Hansel W., Benhelm J., Lancaster G.P.T., Korber T.W., Becher C., Schmidt-Kaler F., James D.F.V., Blatt R. Deterministic quantum teleportation with atoms. *Nature* **429**, 734-737 (2004).
12. K. Hammerer, E.S. Polzik, J.I. Cirac. Teleportation and spin squeezing utilizing multimode entanglement of light with atoms. *Phys. Rev. A* **72**,052313 (2005).

13. L. Vaidman, *Phys. Rev. A* **49**, 1473 (1994)
14. B. Julsgaard, J. Sherson, J. Fiurášek, J.I. Cirac, and E.S. Polzik. Experimental demonstration of quantum memory for light. *Nature*, **432**, 482 (2004)
15. Julsgaard B., Kozhekin A. and Polzik E.S., Experimental long-lived entanglement of two macroscopic objects, *Nature* **413**, 400 (2001).
16. Julsgaard B., Schori C., Sørensen J. L., and Polzik E. S., Atomic spins as a storage medium for quantum fluctuations of light, *Quant. Information and Computation*, **3** special issue, 518 (2003).
17. Julsgaard B., Sherson J., Sørensen J.L., and Polzik E.S., Characterizing the spin state of an atomic ensemble using the magneto-optical resonance method. *J. Opt. B: Quantum and Semiclassical Optics*, **6**, 5 (2004).
18. Sherson J., Julsgaard B., and Polzik E.S., Deterministic atoms-light quantum interface. To appear in *Advances in Atomic, Molecular and Optical Physics*, November 2006. quant-ph/0601186.
19. Chou C.W., Polyakov S.V., Kuzmich A., Kimble H.J. Single-photon generation from stored excitation in an atomic ensemble. *Phys.Rev.Lett.* **92**, 213601 (2004).
20. Chaneliere T., Matsukevich D.N., Jenkins S.D., Lan S.Y., Kennedy T.A.B., Kuzmich A. Storage and retrieval of single photons transmitted between remote quantum memories. *Nature* **438**, 833-836 (2005).
21. Eisaman M.D., Andre A., Massou F., Fleischhauer M., Zibrov A.S., Lukin M.D. Electromagnetically induced transparency with tunable single-photon pulses. *Nature* **438**, 837-841 (2005)

22. Kuhn A., Hennrich M., Rempe G. Deterministic single-photon source for distributed quantum networking. *Phys.Rev.Lett.*, **89**, 067901 (2002).
23. McKeever J., Boca A., Boozer A.D., Miller R., Buck J.R., Kuzmich A., Kimble H.J. Deterministic generation of single photons from one atom trapped in a cavity. *Science* **303**, 1992-1994 (2004).
24. J. S. Neergaard-Nielsen, B. Melholt Nielsen, C. Hettich , K. Mølmer, E. S. Polzik. Generation of a superposition of odd photon number states for quantum information networks. Submitted to *Phys.Rev.Lett.* quant-ph/0602198.
25. The experiment was carried out in the Quantum Optics laboratory at the Niels Bohr Institute, Copenhagen University.

This research has been funded by the Danish National Research Foundation, by EU grants COVAQIAL and QAP, and by the Carlsberg Foundation. I.C. and E.S.P. would like to acknowledge the hospitality of ICFO - Institut de Ciències Fotòniques in Barcelona where ideas leading to this work were first discussed. Permanent address of K.H.: Institut für theoretische Physik, Leopold-Franzens-Universität, Technikerstr. 25, 6020 Innsbruck, Austria

**Correspondence and requests for materials should be addressed to Eugene Polzik,
polzik@nbi.dk**

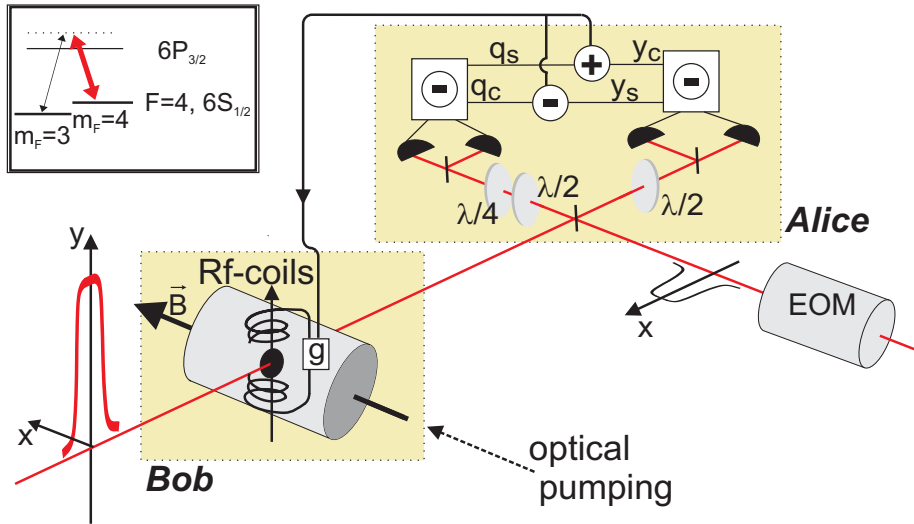


Figure 1. Experimental setup for teleportation of light onto an atomic ensemble. A strong pulse of light (shown on the left) is sent through the atomic sample. After propagating through the sample and becoming entangled with the sample it travels to Alice where it is mixed on a beamsplitter with the input pulse of light – the object of teleportation – generated by the electro-optical modulator (EOM). Two pairs of detectors perform a generalized Bell measurement by measuring polarization operators of light. The results of these measurements are combined, as described in the text, and send via a classical communication channel to Bob, where they are used to complete the teleportation onto atoms by shifting the atomic collective spin state. After a short delay, a second strong pulse - the verifying pulse - is sent to read out the atomic state, in order to prove the successful teleportation.

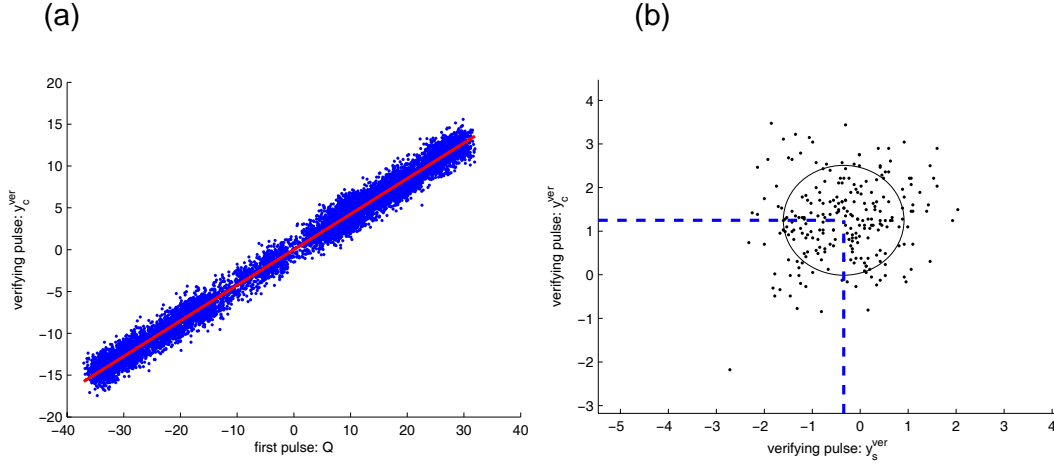


Figure 2. Raw experimental data for a series of teleportation runs. a). Verifying pulse quadrature y_c^{ver} versus the input pulse quadrature Q for 10,000 teleportation runs. The coherent input state has a mean photon number of $\bar{n} \approx 500$ and is slowly modulated in phase during this measurement. The straight line fit is used for calibration of the classical feedback gain (see comments in the text). b). two quadratures of the verifying pulse, y_c^{ver} and y_s^{ver} for a fixed input state with $\bar{n} = 5$. The contour indicates the standard deviation $\sqrt{Var(y_c^{ver}) + Var(y_s^{ver})}$. $Var(y_{c,s}^{ver})$ are used to determine the teleportation fidelity as discussed in the text.

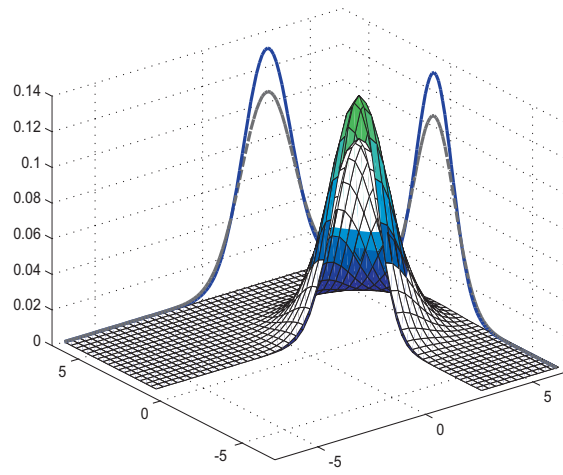


Figure 3. Tomographic reconstruction of a teleported state with $\bar{n} = 5$ (colored contour) versus the state corresponding to the best classical state transfer.

Supplementary Methods.

Projection noise measurement and experimental uncertainties.

The standard deviation of the fidelity in the paper is calculated as follows:

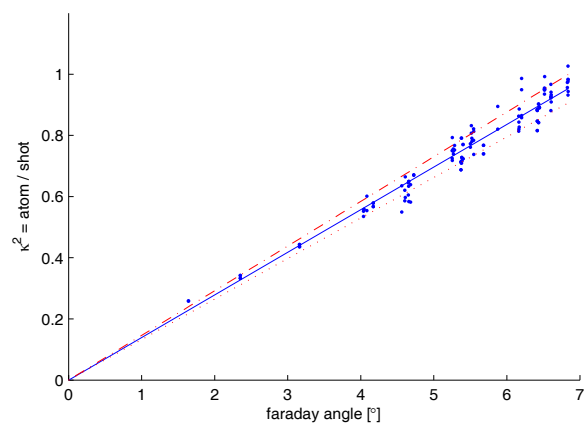
$$SD(F) = \sqrt{\delta_{PN}^2 + \delta_{SN}^2 + \delta_{el}^2 + \delta_{\beta}^2 + \delta_{SNR}^2 + \delta_g^2} =$$

$$= 10^{-2} \sqrt{1.0^2 + 1.65^2 + 0.1^2 + 0.3^2 + 0.2^2 + 0.8^2} \approx 0.02$$

where δ_{PN} is the contribution to the $SD(F)$ due to the projection noise fluctuations, δ_{SN} - the contribution due to the shot noise level uncertainty, δ_{el} - the contribution of the electronics noise level fluctuations, δ_{β} - the uncertainty due to fluctuations in the atomic decay constant, δ_{SNR} - the contribution of the fluctuations in the ratio of responses of two pairs of detectors, and δ_g - is the contribution of the gain fluctuations.

The projection noise and its uncertainty are determined from data presented in the Supplementary Methods figure. The projection noise is taken, as described in the paper, by varying the number of atoms in a two-cell experiment and measuring the noise of the transmitted probe as a function of the Faraday rotation angle proportional to the number of atoms. The plotted variance of the transmitted probe light is normalized to the variance of the shot noise of the probe. Note that the shot noise variance is subtracted, so that the plot goes through the origin. Several experimental runs taken over a time period of a few weeks are collected in the figure to show a good reproducibility of the projection noise level.

The value of κ^2 for a given value of the Faraday angle can be directly read from the figure. The dashed-dotted and dotted lines are the fits used to determine the standard deviation of the projection noise slope.



Supplementary Methods figure

Supplementary Notes

In this section we show (i) how one can relate the teleportation fidelity of coherent states to that of qubits and (ii) how a fidelity approaching unity can be achieved in a more sophisticated teleportation protocol.

(i) Let us call E the (completely positive) map that transforms the state to be teleported to the teleported one. We assume that we know the action of E on coherent states, i.e., $E(|\alpha\rangle\langle\alpha|)$. The goal is to determine the qubit fidelity, F_q , of this map. This is given by $F_q = \int d\Omega \langle\Psi(\Omega)| E(|\Psi(\Omega)\rangle\langle\Psi(\Omega)|) |\Psi(\Omega)\rangle$

where $|\Psi(\Omega)\rangle = \cos(\theta/2)|0\rangle + e^{i\varphi} \sin(\theta/2)|1\rangle$ and the integration is over the 4π solid angle. This expression can be easily determined in terms of

$$\langle a | E(|n\rangle\langle m|) | b \rangle = \frac{1}{\sqrt{n!m!}} \partial_\alpha^n \partial_{\alpha^*}^m \left[e^{|\alpha|^2} \langle a | E(|\alpha\rangle\langle\alpha|) | b \rangle \right] \Big|_{\alpha=0}$$

with $n, m, a, b = 0, 1$. Note that, in practice, one can also determine these quantities in terms of other measurable quantities. In the present experiment, one can characterize E as

$$E(|\alpha\rangle\langle\alpha|) = \frac{1}{2\pi s^2} \int d^2\beta e^{-|\beta - g\alpha|^2/(2s^2)} |\beta\rangle\langle\beta|$$

where $s^2 = 4\sigma^2 - 1$ is related to the atomic variance, σ^2 (which we assumed for simplicity to be the same for X and P) and g is the gain (whose values are restricted given the complete positiveness of E). For this map we obtain

$$F_q = \frac{6 + 16s^2 + 24s^4 + 4(g-1)(1-2s^2) + (g-1)^2(1-6s^2)}{6(1+2s^2)^3}$$

This shows that, in principle, one can obtain arbitrarily high fidelities for $g = 1$ and small variances. For a particular teleportation protocol used in this paper, the value of σ^2 is known, and one obtains a fidelity of 0.74 for $\kappa = 1$, in the absence of losses and decoherence.

(ii) A fidelity approaching unity can be achieved, in principle, by using squeezed light in the entangling pulse and measuring a number of higher order scattering modes in addition to the zero-th order cosine and sine modes. As explained in Ref. 12 of the paper, the input-output relations describing the state of atoms and light after the interaction can be appended by similar relations for higher order modes $[y_{\alpha,n}, q_{\beta,m}] = i\delta_{\alpha\beta}\delta_{nm}$ where $\alpha, \beta = c, s$ and $n, m = 1, 2, \dots$. Note that for the noise operators v_α in Eq. (1) we have $v_\alpha = q_{\alpha,1}$. These modes can easily be measured in the same setup as was used in the current experiment. After the interaction, these modes are transformed as $q_{c(s),n}^{\text{out}} = q_{c(s),n}^{\text{in}}$ and $y_{c(s),n}^{\text{out}} = y_{c(s),n}^{\text{in}} \pm \frac{\kappa^2}{4} (c_n q_{s(c),n-1}^{\text{in}} - c_{n+1} q_{s(c),n+1}^{\text{in}})$ where $c_n = (4n^2 - 1)^{-1/2}$. Extension of the teleportation protocol which includes these modes amounts to preparing the input state in some appropriate linear combination thereof, that is, in a mode $Y = \sum_n g_n \frac{1}{\sqrt{2}} (Y_{s,n} + Q_{c,n})$ and $Q = -\sum_n g_n \frac{1}{\sqrt{2}} (Y_{c,n} - Q_{s,n})$ where $\sum_n g_n^2 = 1$. We numerically checked that for $\kappa > 4$ it is always possible to find real parameters g_n such that the final state of atoms after the feedback is given by $X_A^{\text{tele}} = Y + \frac{1}{\sqrt{2}} \sum_n g_n y_{s,n}^{\text{in}}$ and $P_A^{\text{tele}} = Q + \frac{1}{\sqrt{2}} \sum_n g_n y_{c,n}^{\text{in}}$ corresponding to half a unit of vacuum noise in each spin component or a teleportation fidelity of $F = 0.80$. For this, it is necessary to measure only a number of $n \sim \kappa$ higher order modes. The remaining added noise is due to the vacuum fluctuations of the entangling beam. It is possible to reduce this remaining noise by using a broadband squeezed light, so that the fidelity would approach unity, as the variances of $y_{\alpha,n}^{\text{in}}$ approach zero.